

SCIENTIFIC REPORTS



OPEN

Physical plasma-triggered ROS induces tumor cell death upon cleavage of HSP90 chaperone

Sander Bekeschus¹ , Maxi Lippert¹, Kristina Diepold², Gabriela Chiosis³, Thomas Seufferlein² & Ninel Azoitei²

HSP90 is a ubiquitously expressed molecular chaperone implicated in the correct folding and maturation of a plethora of proteins including protein kinases and transcription factors. While disruption of chaperone activity was associated with augmented cancer cell death and decreased tumor growth both *in vitro* and *in vivo*, the regulation of HSP90 is not clearly understood. Here we report that treatment of cancer cells with cold physical plasma, an emerging and less aggressive tumor therapy, resulted in ROS generation which subsequently triggered the cleavage of HSP90. Notably, cleavage of HSP90 was followed by the degradation of PKD2, a crucial regulator of tumor growth and angiogenesis. Pre-sensitization of cancer cells with subliminal doses of PU-H71, an HSP90 inhibitor currently under clinical evaluation, followed by treatment with cold-plasma, synergistically and negatively impacted on the viability of cancer cells. Taken together, cold-plasma can be used in conjunction with pharmacologic treatment in order to target the expression and activity of HSP90 and the downstream client proteins implicated in various cancer cell capabilities.

Despite continuous advance in medicine, cancer is still a major threat to human society. Accordingly, many new avenues have been explored in the last decades to battle this disease. One of them is the utilization of reactive oxygen species (ROS) as signaling and damaging agents¹. Among others, heat shock proteins (HSPs) are major gatekeepers that regulate ROS-driven apoptosis². As cancer cells often present deregulated apoptosis pathways, HSPs were identified as interesting targets for tumor therapy³. Exposure of cancer cells to ROS generated by ascorbate-driven menadione redox cycling resulted in a partial cleavage of heat shock protein 90 (HSP90) and formation of a 70 kDa fragment⁴. HSP90 is a ubiquitously expressed chaperone implicated in proper folding of various protein kinases, nuclear receptors and transcription factors^{5–7}. By regulating these so-called HSP90 “client” proteins, the chaperone participates in maintaining cellular homeostasis^{8,9}. We recently reported that pharmacological inhibition of HSP90 by PU-H71 was not only associated with augmented cell death and decreased cancer cell proliferation but also lead to destabilization and subsequent proteasomal degradation of protein kinase D2 (PKD2)¹⁰. The serine-threonine kinase PKD2 and its sister isoforms PKD1 and PKD3 belong to the calcium/calmodulin-dependent protein kinase superfamily¹¹ and are activated by various stimuli including phorbol esters, ROS, receptor tyrosine kinases, and hypoxia^{12–14}. PKD2 was shown to be implicated in cancer cell growth, migration, invasion, and angiogenesis^{14–16}.

ROS are not only generated as metabolic byproducts but also in many physical therapies for medicine such as ionization radiation and photodynamic therapy¹⁷. A recently emerging technology for ROS-based therapy is cold physical plasma. Plasmas are generated by energizing gases leading to partial ionization (dissociation of highly energetic electrons) and often high temperatures. Technical advance led to generation of so-called cold physical plasmas. These multicomponent systems comprise of electrical fields, multitude light emission, ions and electrons, and reactive species. The latter are assumed to be the main driver in anticancer effects of plasma treatment. Exposure to plasma led to induction of cell growth arrest in colorectal cancer¹⁸ and apoptosis in glioblastoma, colon carcinoma, breast cancer, and melanoma^{18–20}. Other reports showed that exposure of Jurkat cells to cold-plasma resulted in the activation of pro-proliferative signaling molecules such as ERK1/2 and MEK1/2²¹.

¹ZIK plasmatis, Leibniz Institute for Plasma Science and Technology (INP Greifswald), Felix-Hausdorff-Str. 2, 17489, Greifswald, Germany. ²Center for Internal Medicine I, University Hospital of Ulm, Albert-Einstein-Allee 23, 89081, Ulm, Germany. ³Department of Molecular Pharmacology and Chemistry, Memorial Sloan-Kettering Institute New York, New York, NY, USA. Maxi Lippert and Kristina Diepold contributed equally. Correspondence and requests for materials should be addressed to S.B. (email: sander.bekeschus@inp-greifswald.de) or N.A. (email: ninel.azoitei@uni-ulm.de)

Sensing *et al.*, proposed that generation of reactive oxygen species (ROS) after cold-plasma treatment induces apoptosis²². Indeed, it has been shown that ROS are harmful to cells by inducing senescence, cell cycle arrest and apoptosis²³. All these results urge thorough investigation of the intimate molecular mechanisms triggering various cellular events by cold-plasma.

The aim of this study was to investigate the molecular mechanism behind the cell death triggered by cold plasma treatment. Our work shows that cold-plasma seems to orchestrate molecular signals in epithelial tumors involving HSP90 chaperone and its client PKD2. Moreover, these data indicate that HSP90 inhibitors such as PU-H71, currently under clinical evaluation in patients, synergize at subliminal doses with cold plasma treatment toward impaired tumor cell viability.

Material and Methods

Cell lines. MDA-MB-231, SW480, MCF-7, PC3 and NCF3 cancer cell lines were cultured either in DMEM or RPMI1640 medium supplemented with 10% fetal bovine serum, 2% glutamine, and 1% penicillin/streptomycin (all Sigma, Germany). Cancer cell lines were obtained from DSMZ—German Collection of Microorganisms and culture cells (Braunschweig, Germany) or authenticated at the Multiplexion (Heidelberg, Germany). For subsequent experiments, cells were pre-incubated with either 50 nM of the pharmacological inhibitor of HSP90 8-[(6-iodo-1,3-benzodioxol-5-yl) sulfanyl]-9-[3-(propan-2-ylamino) propyl] purin-6-amine inhibitor PU-H71 or vehicle control for 4 h. PU-H71 was synthesized and characterized as previously reported²⁴.

Plasmids and lentiviral transduction. The pLenti6.2-V5-DEST-PKD2 over-expression vectors were generated using the pDONR-223-PKD2 entry clone from Addgene (PKD2, #23490). Knock-down of HSP90 β was achieved using an HSP90-specific shRNA (#TRCN000008748) from Open Biosystems. High-titer virus-containing supernatants of HEK 293FT cells after co-transfection of lentiviral vectors with pMD2.G and psPAX2 packaging plasmids were used for lentiviral-mediated transduction of cancer cells.

Plasma treatment. For plasma treatment, 1×10^5 cells were added per well in 24 well plates (Eppendorf, Germany) and allowed to adhere overnight. As plasma source, an atmospheric pressure argon plasma jet kINPen 11 (neoplas, Germany) was used (Fig. 1A). The kINPen 11 is technically similar to the kINPen MED that received approval as medical product for skin diseases. Argon gas (99.9999% pure; Air Liquide, France) was used to ignite the plasma that subsequently generated reactive species in the ambient air (Fig. 1B). The jet was hovered over the cells for the respective amount of time with a computer-programmed xyz-table (CNC, Germany).

Detection of intracellular ROS. In the presence of ROS, the non-fluorescent CM-H₂DCF-DA is converted to the green fluorescent form, when acetate groups are removed by intracellular esterases and intracellular oxidation occurs. Five micromolar of CM-H₂DCF-DA (Thermo Fisher, USA) was added to the adherent cells. After 15 min of incubation, the extracellular dye was washed away. Cell cultures were subjected to plasma treatment. Bright field, digital phase contrast, and fluorescence were imaged using a high-content imaging device (Operetta CLS; PerkinElmer, Germany) with several fields of view per well using a 20x objective (Zeiss, Germany). Several thousand cells per condition were segmented upon signals in digital phase contrast images, and mean fluorescence intensity (MFI) per cell and well was analyzed using Harmony 4.6 software (PerkinElmer).

Measurement of cell viability. Cell viability was assessed by incubating the cells in control and sample wells with 7-hydroxy-3H-phenox-azin-3-one-10-oxide (resazurin, final concentration 100 μ M; Alfa Aesar, USA) for 4 h. In metabolically active cells, resazurin diffuses into the cells and is reduced to fluorescent resorufin. Fluorescence was quantified by using a microplate reader at λ_{ex} 535 nm and λ_{em} 590 nm (Tecan, Switzerland).

Western blot analysis. Whole cell extracts were prepared using a lysis buffer containing 10 mM Tris-HCl, 5 mM EDTA, 50 mM NaCl, 50 mM NaF and 1% Triton X100 supplemented with Complete Protease inhibitor Cocktail (Roche). Lysates were subjected to SDS-PAGE and proteins transferred to PVDF membranes (Millipore, Massachusetts, USA). Membranes were blocked with 5% non-fat dry milk in phosphate buffered saline (PBS) containing 0.2% Tween 20 and incubated overnight at 4 °C with specific antibodies. For subsequent washes 0.2% Tween 20 in PBS was used. The following antibodies were used: HSP90 β (D-19; Santa Cruz Biotechnology, #sc-1057), PKD2 (Bethyl Laboratories, #A300-073A), cleaved PARP (Cell Signaling, #9542S), and β -actin (Sigma, #A1978).

Tumor spheroids. 3×10^3 MDA-MB-231 cells were seeded in ultra-low-affinity round bottom plates (PerkinElmer), centrifuged, and grown for 72 h. Tumor spheroids were left untreated or exposed to plasma. After 24 h, 200 nM Sytox green (Life technologies, USA) was added and 15 z-stacks were imaged per well and spheroid. Using quantitative image analysis, spheroids stacks were merged into maximum intensity projections, segmented, and mean fluorescent intensity of Sytox green within spheroid area was assessed. Sytox green is a cell membrane-impermeable dye that enters only terminally dead cells to exhibit a strong fluorescence increase upon binding to DNA. Hence, it functions similar to e.g. propidium iodide (but with a different spectral properties) to stain dead cells.

Statistical analysis. Statistical analysis as well as graphing was accomplished using Prism 7.03 (GraphPad Software, USA). Mean and statistical significance were calculated and analyzed using *t*-test. Levels of significances were indicated as follows: **p* = 0.05, ***p* = 0.01, ****p* = 0.001. *p* < 0.05 was considered significant. All data are representative of at least three experiments.

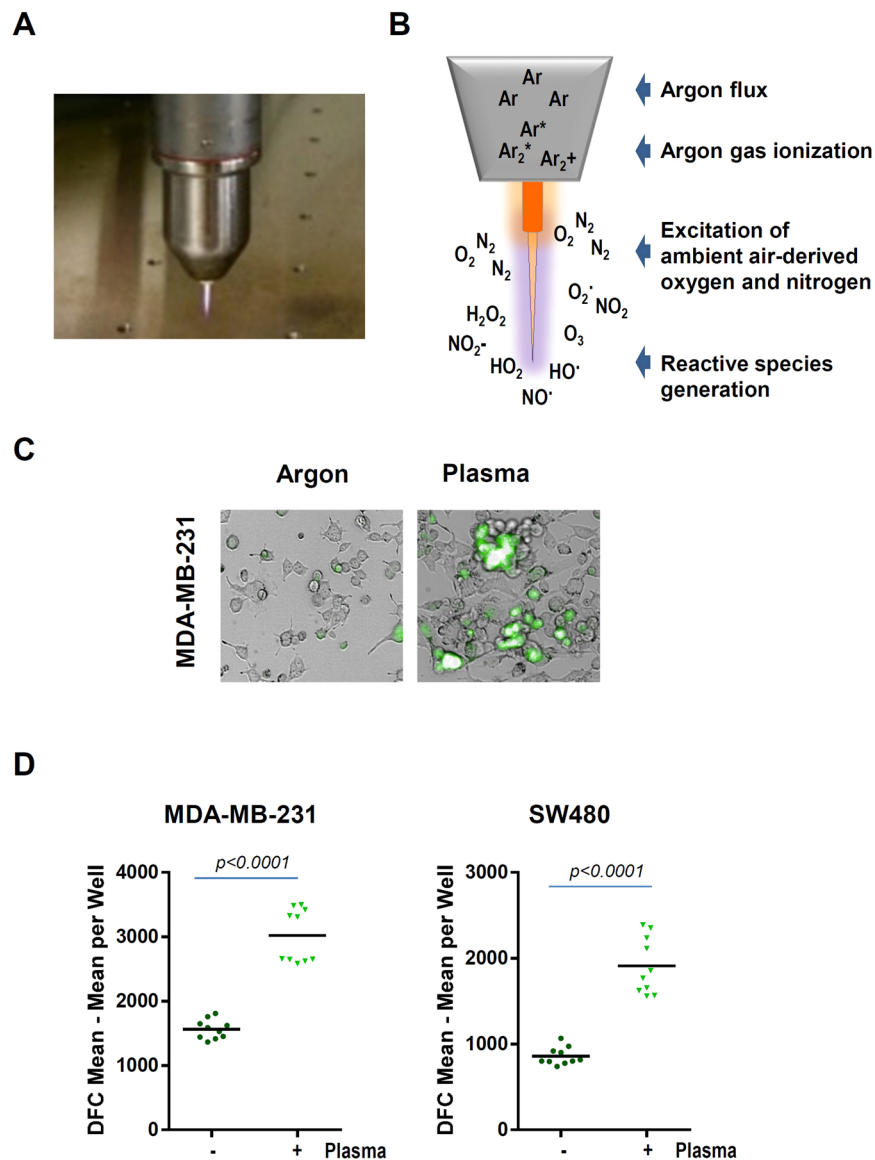


Figure 1. (A,B) The atmospheric pressure argon plasma jet kINPen and principle of reactive species generation. (C) Representative images of redox-sensitive dye CM-H₂DCF-DA-loaded MDA-MB-231 cells in control and plasma-treated samples. (D) Quantitative image analysis of mean fluorescence intensity of the CM-H₂DCF-DA redox-sensitive dye. Plasma treatment time was 60 seconds, image acquisition was performed 1 hour after plasma treatment.

Results

Plasma-derived reactive species impair viability and augment cancer cell death. Cold physical plasma is generated by an atmospheric pressure plasma jet (Fig. 1A). The plasma produces reactive species by ionizing a flow of argon gas that subsequently reacts with ambient air oxygen and nitrogen to form gas-phase reactive oxygen and nitrogen species (ROS/RNS), respectively (Fig. 1B). Cancer cells loaded with an intracellular fluorescent indicator of reactive species turnover were exposed to plasma, and cellular fluorescence was acquired (Fig. 1C). Quantification revealed significantly higher levels of intracellular ROS in plasma-treated cancer cells (Fig. 1D). Next, we investigated the effect of plasma intervention in the viability of various cancer cells. Resazurin assay demonstrated that treatment of cancer cells with plasma resulted in impaired survival as demonstrated by reduced transformation to pink resofurin (Fig. 2A). Furthermore, exposure of MDA-MB-231 breast and SW480 colon cancer cells to plasma jet-generated oxidative stress was associated with decreased viability (Fig. 2B). These results were substantiated in experiments with tumor spheroids (Suppl. Fig. 1). Capan1 pancreatic cancer cells showed resistance to plasma treatment, (Fig. 2B), very likely due elevated levels of SOD and decreased levels of CAT in these cells. In addition, western blot analysis with the apoptosis marker cleaved PARP, demonstrated that decreased cancer cell viability was paralleled by augmented cancer cell death (Fig. 2C).

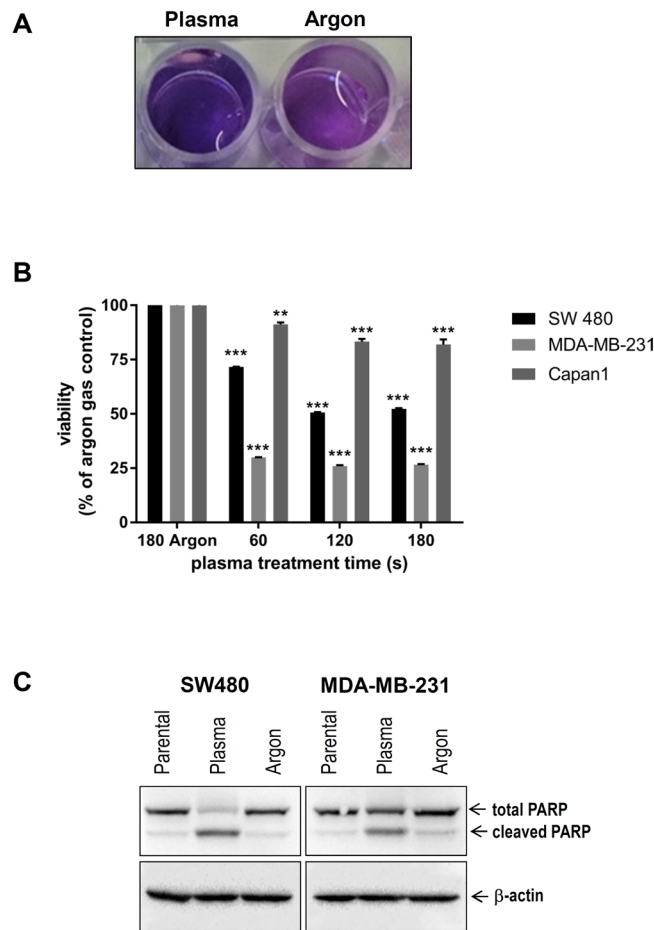


Figure 2. Cold plasma treatment results in impaired cancer cell viability and augmented apoptosis. (A) Representative image of resazurin assay, plasma treatment reduced transformation to pink resofurin indicated decrease in viability 24 hours after plasma treatment. (B) Viability of SW480, MDA-MB-231, and Capan1, respectively. For each cell line, statistical comparison (one-way analysis of variance with Dunnett post-test) of each plasma treatment time (60 s, 120 s, 180 s) compared to argon gas control (180 s) revealed significant ($p < 0.01$ or $p < 0.001$) differences. (C) Twenty-four hours following argon gas or plasma treatment (both 60 s), lysates of MDA-MB-231 and SW480 were subjected to SDS-PAGE followed by incubation with PARP antibodies. β -actin was used as loading control.

HSP90 is cleaved after treatment of cancer cells with cold plasma. HSP90, a cytoplasmic chaperone highly expressed in various cancers, has been reported to play an essential role in buffering stress conditions within the tumor microenvironment²⁵. Beck and colleagues reported that exposure of cancer cells to ROS generated by ascorbate-driven menadione redox cycling resulted in cleavage of HSP90⁴. Interestingly, western blot analysis with lysates from various cancer cells treated with cold plasma, also revealed the same 70 kDa band (Fig. 3A–D), in line with the data of Beck and colleagues⁴. These results suggest that the chaperone is partially cleaved by the ROS generated upon plasma treatment which might be a potential tool in future cancer therapies. We previously reported that pharmacologic inhibition of HSP90 triggered proteasome-dependent degradation of PKD2¹⁰, a protein “client” involved in promoting cancer development. Interestingly, treatment of cancer cells with cold plasma not only resulted in cleavage of HSP90, but was also associated with PKD2 degradation (Fig. 3A–D). These results suggest that HSP90 cleavage-driven PKD2 degradation may contribute to the impaired proliferation and augmented cancer cell death observed after plasma treatment (Fig. 2A–C). Interestingly, cell death level following plasma treatment was comparable to that achieved upon lentiviral-mediated HSP90 knock-down (Suppl. Fig. 2A,B).

Treatment with cold plasma boosts cell death in pharmacologically pre-sensitized cancer cells. Since HSP90 specifically maintains proper folding and function of various proteins mutated or over-expressed in human cancer^{25–27}, several ATP-competitive HSP90 inhibitors are under clinical investigation^{28–30}. Therefore, we sought to involve an HSP90 inhibitor, currently in the clinical trials, in a combined therapy with cold-plasma. Our previous studies showed that treatment of various cancer cells with 0.5 to 1 μ M PU-H71 resulted in augmented cell death^{10,31,32}. Here, we pre-incubated MDA-MB-231 breast and SW480 colon cancer cells with as little as 50 nM PU-H71 before plasma intervention. At this concentration, western blot analysis with cleaved PARP revealed no difference in cell death compared to untreated cells (Fig. 4A,B). On the other hand, 30 seconds cold-plasma

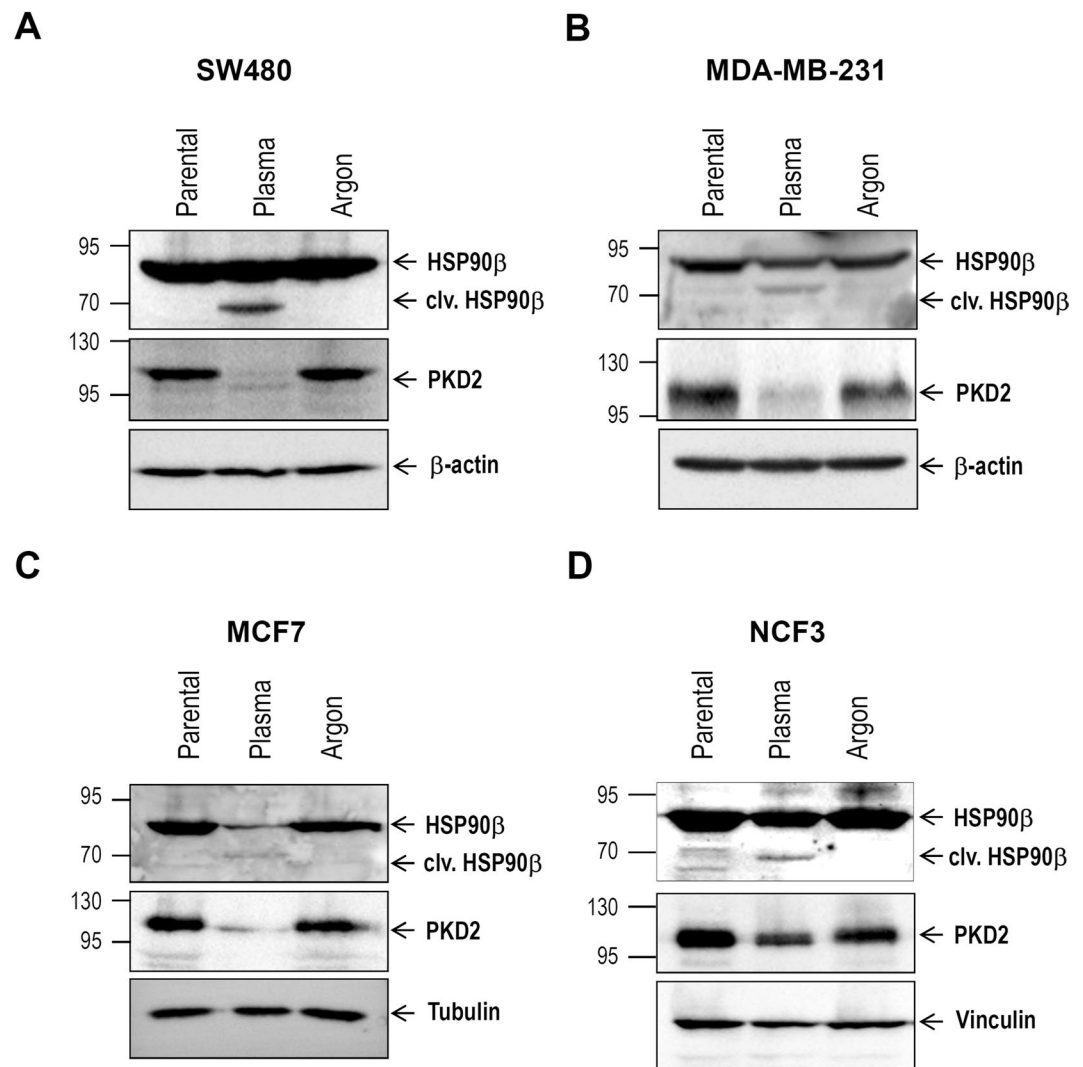


Figure 3. Cold plasma treatment is associated with cleavage of HSP90 chaperone and PKD2 degradation. (A–D) Various cancer cell lines were subjected to treatment with plasma jet (60 s). Twenty-four hours later, cleared lysates were used for western blot analysis in order to determine the HSP90 and PKD2 abundance.

treatment substantially reduced cancer cell viability (Fig. 4C–F). Most important, pre-sensitization of cancer cells with 50 nM PU-H71 was sufficient to significantly boost cell death triggered by cold-plasma therapy with up to around 60% (Fig. 4C–F). These results indicate a synergistic effect between the two therapies targeting the chaperone.

Ectopic PKD2 is not sufficient to restore cancer cell viability after combined therapy. Given that HSP90 inhibition results in decreased tumor growth in a PKD2-dependent manner¹⁰, we sought to investigate the magnitude of the kinase participation to cell death triggered through a combined intervention. Cancer cells transfected with an expression vector encoding PKD2 (PKD2 o.e.) or empty vector (PKD2 e.v.) (Fig. 5A) were subjected to pre-incubation with 50 nM PU-H71 for 24 hours before treatment with cold-plasma. Our results show that simple PKD2 over-expression is not enough to rescue cell viability after combined drug and plasma therapy (Fig. 5B,C). These results indicate that cell death following combined plasma and drug treatment is not a lone result of HSP90 cleavage and PKD2 degradation, respectively, as additional molecular mechanisms or molecules likely contribute to this cellular event as well. Investigation of another kinase reported to act as an HSP90 client, namely serine/threonine-kinase 33 (STK33)^{31,32}, showed that cold-plasma treatment was also associated with STK33 degradation (Suppl. Figs 2B and 3A). The fact that PKD2 and STK33 represent just two of around 200 client proteins described until now for the chaperone, may very well reason the lack of restored viability after ectopic PKD2 expression alone.

Discussion

Most existing drugs designed to target and kill cancer cells are harmful and poisonous to the human body as they also attack non-malignant cells, thus triggering serious side effects. Therefore, scientists are set to tailor and combine new therapies, less aggressive and invasive. In the last decade, several reports successfully documented the implication of cold-plasma in treatment of various tumors. While the results are promising, the intimate molecular mechanism of how cold-plasma therapy impacts on tumor cell viability remains elusive to date.

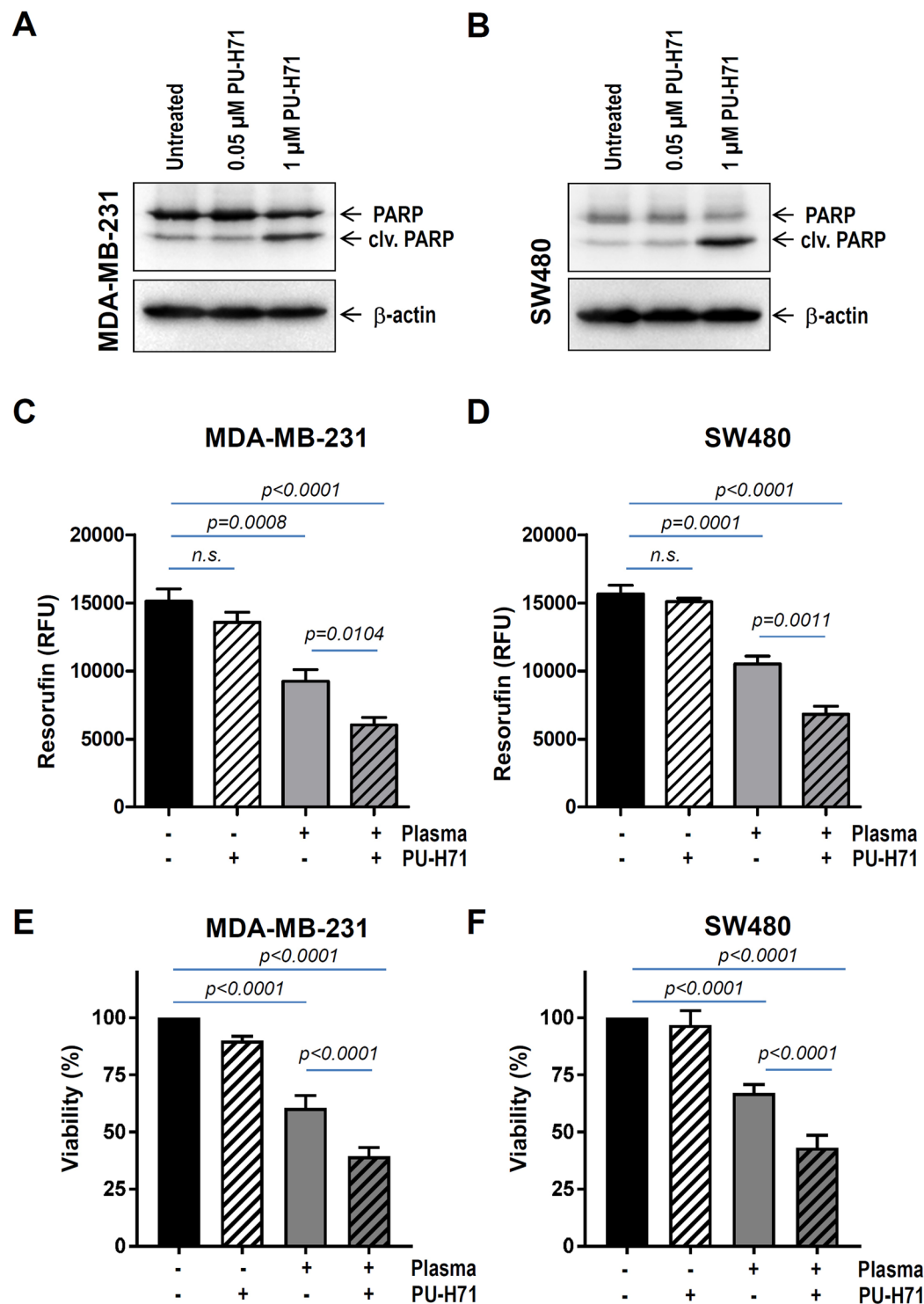


Figure 4. Cold plasma treatment boosts cell death in drug pre-sensitized cancer cells. (A) MDA-MB-231 breast and (B) SW480 colon cancer were treated for 24 hours with HSP90 inhibitor as indicated. Apoptosis was determined by examining the levels of cleaved PARP in western blot analysis. (C,E) MDA-MB-231 and (D,F) SW480 cancer cells were either incubated with 50 nM PU-H71 or subjected to plasma treatment (60 s) or both. A synergistic toxicity between PU-H71 and plasma treatment was observed at 24 h. RFU = relative fluorescence units.

In this study we have demonstrated that treatment of cancer cells with cold-plasma results in generation of ROS, which negatively impacts on tumor cell proliferation and viability. Furthermore, plasma-driven ROS triggered the cleavage of HSP90 chaperone and subsequent degradation of its client PKD2, previously shown to be essential for cancer cell proliferation and viability. Finally, our study revealed that combined therapy using sub-minimal doses of HSP90 inhibitor and cold-plasma treatment was associated with decreased viability of cancer cells.

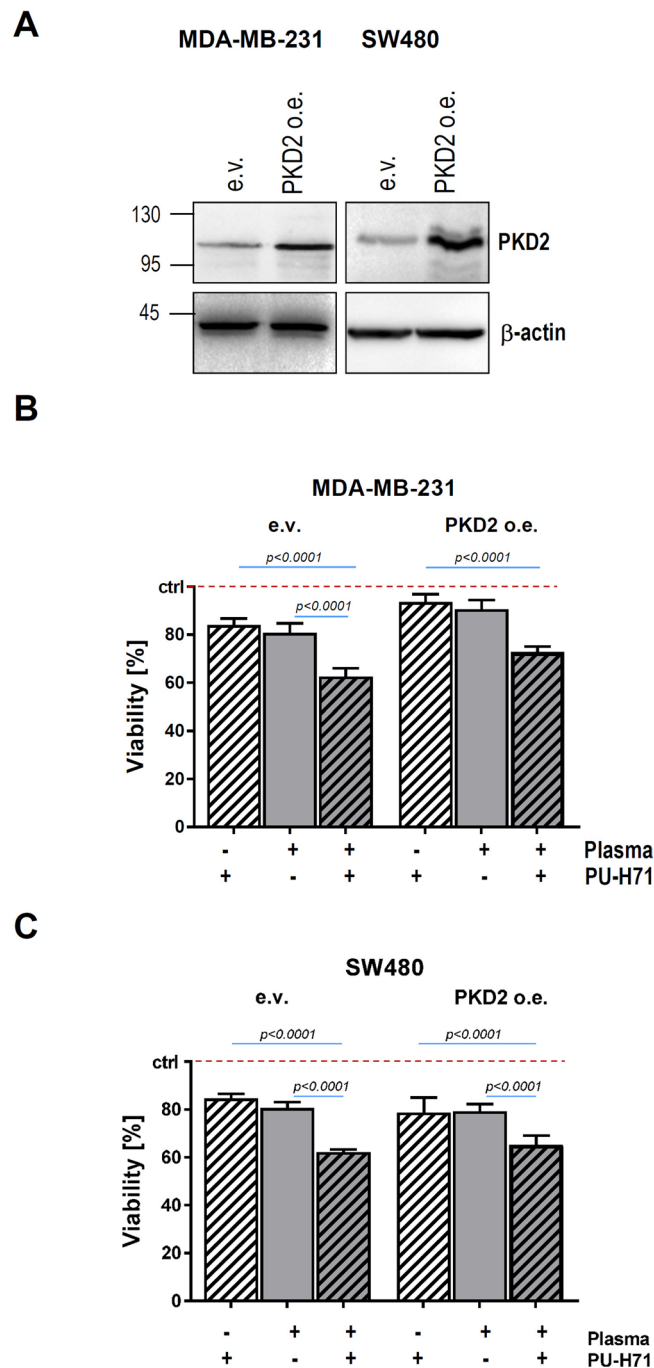


Figure 5. Ectopic PKD2 expression is not sufficient to restore cancer cell viability after treatment with cold plasma. Cancer cells were transduced with a PKD2 expression (PKD2 o.e.) or empty vector (e.v.). After selection with antibiotic, lysates of transduced cancer cells were prepared and SDS-PAGE was conducted with PKD2 antibody. β -actin was used as loading control. (B,C) MDA-MB-231 breast and SW480 colon cancer cells (e.v. as well as PKD2 o.e.) were treated with plasma (60 s) and/or 50 nM PU-H71, and cell viability was determined at 24 h.

Cold physical plasmas are multicomponent systems with potential biological impact from e.g. UV and mild thermal radiation, electrons and ions, electric fields, and ROS/RNS. However, for effects in *in vitro* cultures, only few can be held accountable for the results observed. The UV-C portion of plasma penetrates liquids only 100 nm in depths³³, thus cells underneath cell culture liquid are protected. The distance plasma-derived solvated electrons can travel in liquids is even lower and in the range of 2 nm³⁴. Although the presence of positive ions in the gas phase of the plasma effluent has been directly shown³⁵, measurements of solvated ions into the liquid (and their subsequent biological effects) is technically challenging. For thermal radiation, the jet was measured to have 37 °C at the tip of the effluent, making non-physiological heating of cells during plasma treatment unlikely. When the jet is operated in ambient air surrounding the plasma, electric fields contribute to its propagation to a minimal

Plasma therapy

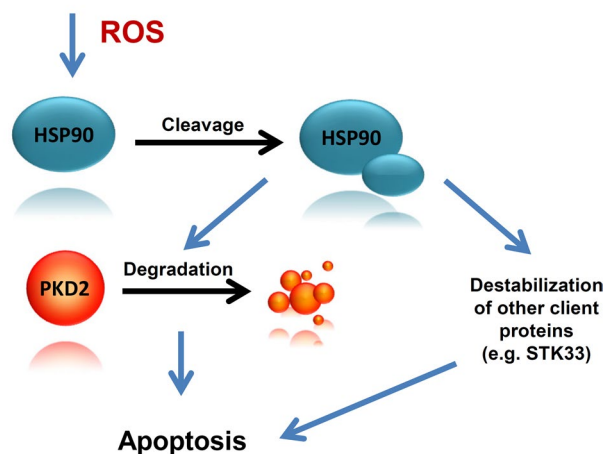


Figure 6. Cleavage of HSP90 and degradation of PKD2 following cold plasma treatment is associated with cancer cell death. Physical plasma treatment-generated ROS is followed by HSP90 cleavage and subsequent destabilization and degradation of PKD2. While PKD2 degradation plays an important role in cancer cell death, additional essential molecules such as STK33, also contribute to the apoptotic event. Furthermore, pre-treatment of cancer cells with subliminal doses of HSP90 inhibitor followed by cold plasma treatment boosts cell death in human cancer.

extent only³⁶. Hence, while all of the above plasma parameters in principle are capable of having an impact on cells, their role in our setup is negligible. By contrast, ROS/RNS were shown to be the prime contributor in plasma-treated cells *in vitro*^{37–39}.

HSP90 orchestrates the stabilization and activation of around 200 protein clients, many of which are oncoproteins required for the acquisition and maintenance of the major cancer hallmarks. This renders HSP90 to be a crucial target when developing new strategies and drugs to inhibit chaperone's activity and induce cancer cell death through the destabilization of client proteins. Beck and colleagues were able to provoke the oxidative cleavage of HSP90 upon generation of ROS by a Fenton-type reaction in proximity to the N-terminal nucleotide binding site of the chaperone⁴. The cleavage is biologically relevant as it was followed by K562 cell death⁴. The fact that cold-plasma generates ROS, for instance superoxide, peroxide and hydroxyl radicals⁴⁰ prompted us to investigate, whether treatment of cancer cells with cold-plasma results in the cleavage of chaperone. To our best knowledge, this work is the first to show that cold-plasma treatment is associated with HSP90 cleavage. *In vitro* treatment of colon, prostate and breast cancer cells with cold-plasma resulted in 70 kDa fragment, in line with the previous data⁴. The next question was whether cleavage of HSP90 at the crucial site in the N-terminus responsible for chaperone's activity, was associated with client degradation. Indeed, treatment with cold-plasma was associated with the degradation of PKD2, a protein shown in our laboratory to act as a HSP90 client¹⁰. These results suggest that one mechanism, by which cell death is promoted after plasma treatment, is represented by ROS-induced HSP90 cleavage and subsequent PKD2 degradation (Fig. 6). Intriguingly enough, cell death triggered by plasma-induced HSP90 cleavage-induced PKD2 destabilization was not restored by overexpressing PKD2. This suggests that additional chaperone client proteins might be involved in this process. Our investigations show that at least one additional client of HSP90, namely STK33, is involved in this scenario as plasma treatment also triggered its degradation (Fig. 6). The very likely involvement of many other client proteins in the cell death following HSP90 cleavage by plasma, reasons the lack of viability rescue in our experimental setup after attempting to overexpress PKD2 only. To note, cleavage of HSP90/degradation of PKD2 is only one within several molecular events following delivery of cold-plasma to cancer cells. Many of these death-triggering molecular events are not known or are barely understood.

Our recent results show that as less as 1 μ M PU-H71 is sufficient to promote cell death as a result of HSP90 inhibition-triggered client degradation^{10,31,32}. In an attempt to mimic sub-liminal drug doses in clinical setup we used for further experiments 50 nM PU-H71. At this concentration no cell death was detected upon cleaved PARP analysis. However, 50 nM was sufficient to sensitize cancer cells to plasma therapy, so that a synergistic effect between drug and plasma was achieved. This finding favours targeting HSP90 in a combinatorial therapy.

However, future studies using more tumor types and *in vivo* animal models are needed to provide information about the generalization of our finding and its relevance in biological systems.

References

1. Trachootham, D., Alexandre, J. & Huang, P. Targeting cancer cells by ROS-mediated mechanisms: a radical therapeutic approach? *Nat Rev Drug Discov.* **7**, 579–91 (2009).
2. Lanneau, D. *et al.* Heat shock proteins: essential proteins for apoptosis regulation. *J Cell Mol Med.* **3**, 743–61 (2008).
3. Sreedhar, A. S. & Csermely, P. Heat shock proteins in the regulation of apoptosis: new strategies in tumor therapy: a comprehensive review. *Pharmacol Ther.* **101**, 227–57 (2004).

4. Beck, R. *et al.* Hsp90 is cleaved by reactive oxygen species at a highly conserved N-terminal amino acid motif. *PLoS One*. **7**, e40795 (2012).
5. McClellan, A. J. *et al.* Diverse cellular functions of the Hsp90 molecular chaperone uncovered using systems approaches. *Cell*. **131**, 121–35 (2007).
6. Picard, D. Heat-shock protein 90, a chaperone for folding and regulation. *Cell Mol Life Sci*. **59**, 1640–1648 (2002).
7. Abbas-Terki, T., Briand, P. A., Donzé, O. & Picard, D. The Hsp90 co-chaperones Cdc37 and Sti1 interact physically and genetically. *Biol Chem*. **383**, 1335–1342 (2002).
8. Whitesell, L., Bagatell, R. & Falsey, R. The stress response: implications for the clinical development of hsp90 inhibitors. *Curr Cancer Drug Targets*. **3**, 349–58 (2003).
9. Caplan, A. J., Mandal, A. K. & Theodoraki, M. A. Molecular chaperones and protein kinase quality control. *Trends Cell Biol*. **17**, 87–92 (2007).
10. Azoitei, N. *et al.* HSP90 supports tumor growth and angiogenesis through PRKD2 protein stabilization. *Cancer Res*. **74**, 7125–7136 (2014).
11. Manning, G., Whyte, D. B., Martinez, R., Hunter, T. & Sudarsanam, S. The protein kinase complement of the human genome. *Science*. **298**, 1912–1934 (2002).
12. Rykx, A. *et al.* Protein kinase D: a family affair. *FEBS Lett*. **546**, 81–86 (2003).
13. Storz, P. Mitochondrial ROS eradicant detoxification, mediated by protein kinase D. *Trends Cell Biol*. **17**, 13–18 (2007).
14. Azoitei, N. *et al.* Protein kinase D2 is a crucial regulator of tumour cell-endothelial cell communication in gastrointestinal tumours. *Gut*. **59**, 1316–1330 (2010).
15. Bernhart, E. *et al.* Protein kinase D2 regulates migration and invasion of U87MG glioblastoma cells *in vitro*. *Exp Cell Res*. **319**, 2037–2048 (2013).
16. Wille, C. *et al.* Protein kinase D2 induces invasion of pancreatic cancer cells by regulating matrix metalloproteinases. *Mol Biol Cell*. **25**, 324–336 (2014).
17. Garg, A. D., Krysko, D. V., Vandenabeele, P. & Agostinis, P. DAMPs and PDT-mediated photo-oxidative stress: exploring the unknown. *Photochem Photobiol Sci*. **10**, 670–680 (2011).
18. Kim, C. H. *et al.* Induction of cell growth arrest by atmospheric non-thermal plasma in colorectal cancer cells. *J Biotechnol*. **150**, 530–538 (2010).
19. Vandamme, M. *et al.* ROS implication in a new antitumor strategy based on non-thermal plasma. *Int J Cancer*. **130**, 2185–2194 (2012).
20. Binenbaum, Y. *et al.* Cold Atmospheric Plasma, Created at the Tip of an Elongated Flexible Capillary Using Low Electric Current, Can Slow the Progression of Melanoma. *PLoS One*. **12**, e0169457 (2017).
21. Bundscherer, L. *et al.* Impact of non-thermal plasma treatment on MAPK signaling pathways of human immune cell lines. *Immunobiology*. **218**, 1248–1255 (2013).
22. Sensenig, R. *et al.* Non-thermal plasma induces apoptosis in melanoma cells via production of intracellular reactive oxygen species. *Ann Biomed Eng*. **39**, 674–687 (2011).
23. Lehnert, B. E. & Iyer, R. Exposure to low-level chemicals and ionizing radiation: reactive oxygen species and cellular pathways. *Hum Exp Toxicol*. **21**, 65–69 (2002).
24. Rodina, A. *et al.* The epichaperome is an integrated chaperome network that facilitates tumour survival. *Nature*. **538**, 397–401 (2016).
25. Taipale, M., Jarosz, D. F. & Lindquist, S. HSP90 at the hub of protein homeostasis: emerging mechanistic insights. *Nat Rev Mol Cell Biol*. **11**(7), 515–28 (2010). Jul.
26. Gorre, M. E., Ellwood-Yen, K., Chiosis, G., Rosen, N. & Sawyers, C. L. BCR-ABL point mutants isolated from patients with imatinib mesylate-resistant chronic myeloid leukemia remain sensitive to inhibitors of the BCR-ABL chaperone heat shock protein 90. *Blood*. **100**, 3041–3044 (2002).
27. Cerchietti, L. C. *et al.* A purine scaffold Hsp90 inhibitor destabilizes BCL-6 and has specific antitumor activity in BCL-6-dependent B cell lymphomas. *Nat Med*. **12**, 1369–1376 (2009).
28. Whitesell, L. & Lindquist, S. L. HSP90 and the chaperoning of cancer. *Nat Rev Cancer*. **5**, 761–772 (2005).
29. Wang, Y., Trepel, J. B. & Neckers, L. M. Giaccone G. STA-9090, a small-molecule Hsp90 inhibitor for the potential treatment of cancer. *Curr Opin Investig Drugs*. **11**, 1466–1476 (2010).
30. Moullick, K. *et al.* Affinity-based proteomics reveal cancer-specific networks coordinated by Hsp90. *Nat Chem Biol*. **7**, 818–826 (2011).
31. Azoitei, N. *et al.* Targeting of KRAS mutant tumors by HSP90 inhibitors involves degradation of STK33. *J Exp Med*. **209**, 697–711 (2012).
32. Liu, Y. *et al.* STK33 participates to HSP90-supported angiogenic program in hypoxic tumors by regulating HIF-1 α /VEGF signaling pathway. *Oncotarget*. **8**, 77474–77488 (2017).
33. Jablonowski, H. *et al.* Impact of plasma jet vacuum ultraviolet radiation on reactive oxygen species generation in bio-relevant liquids, *Physics of Plasmas*, **22**, id.122008 (2015).
34. Rumbach, P., Bartels, D. M., Sankaran, R. M. & Go, D. B. The solvation of electrons by an atmospheric-pressure plasma. *Nat Commun*. **6**, 7248 (2015).
35. Dünnbier, M. *et al.* Ambient air particle transport into the effluent of a cold atmospheric-pressure argon plasma jet investigated by molecular beam mass spectrometry *Journal of Physics D: Applied Physics*. **46** (2013).
36. Ansgar Schmidt-Bleker, S. A. *et al.* Propagation mechanisms of guided streamers in plasma jets: the influence of electronegativity of the surrounding gas *Plasma Sources Science and Technology*, **24** (2015).
37. Ahn, H. J. *et al.* Atmospheric-pressure plasma jet induces apoptosis involving mitochondria via generation of free radicals. *PLoS One*. **6**, e28154 (2011).
38. Liedtke, K. R. *et al.* Cold Physical Plasma Selectively Elicits Apoptosis in Murine Pancreatic Cancer Cells *In Vitro* and *In Ovo*. *Anticancer Res*. **38**, 5655–5663 (2018).
39. Adachi, T. *et al.* Plasma-activated medium induces A549 cell injury via a spiral apoptotic cascade involving the mitochondrial-nuclear network. *Free Radic Biol Med*. **79**, 28–44 (2015).
40. Jawaid, P. *et al.* Helium-based cold atmospheric plasma-induced reactive oxygen species-mediated apoptotic pathway attenuated by platinum nanoparticles. *J Cell Mol Med*. **20**, 1737–1748 (2016).

Acknowledgements

The authors gratefully acknowledge technical support by Felix Nießner and Juliane Moritz. This work was supported by the German Federal Ministry of Education and Research (BMBF, grant number 03Z22DN11 to S.B. and M.L.) and the German Research Foundation (DFG, grant AZ.96/1-3 to NA). G.C. is supported in part by the US National Institutes of Health (NIH) (R01 CA172546, R56 AG061869, R01 CA155226, P01 CA186866, P30 CA08748 and P50 CA192937).

Author Contributions

N.A. and S.B. wrote the main manuscript text and prepared the figures. M.L. and K.D. conducted the experiments. G.C. provided the HSP90 inhibitor. T.S. critically reviewed the manuscript. All authors reviewed the manuscript.

Additional Information

Supplementary information accompanies this paper at <https://doi.org/10.1038/s41598-019-38580-0>.

Competing Interests: Memorial Sloan-Kettering Cancer Center holds the intellectual rights to PU-H71. Samus Therapeutics, of which G. Chiosis has partial ownership, has licensed PU-H71. The corresponding authors are responsible for submitting on behalf of all authors of the paper.

Publisher's note: Springer Nature remains neutral with regard to jurisdictional claims in published maps and institutional affiliations.



Open Access This article is licensed under a Creative Commons Attribution 4.0 International License, which permits use, sharing, adaptation, distribution and reproduction in any medium or format, as long as you give appropriate credit to the original author(s) and the source, provide a link to the Creative Commons license, and indicate if changes were made. The images or other third party material in this article are included in the article's Creative Commons license, unless indicated otherwise in a credit line to the material. If material is not included in the article's Creative Commons license and your intended use is not permitted by statutory regulation or exceeds the permitted use, you will need to obtain permission directly from the copyright holder. To view a copy of this license, visit <http://creativecommons.org/licenses/by/4.0/>.

© The Author(s) 2019